ISSN (Online) 2321 – 2004
ISSN (Print) 2321 – 5526

INTERNATIONAL JOURNAL OF INNOVATIVE RESEARCH IN ELECTRICAL, ELECTRONICS, INSTRUMENTATION AND CONTROL ENGINEERING
Vol. 2, Issue 4, April 2014

Noise Modelling of Atmospheric Radar Data using Empirical Mode Decomposition

Uma Maheswara Rao D[1], T. Sreenivasulu Reddy[2], G. Ramachandra Reddy[3]

Abstract: In this paper, we model the noise present in middle and upper layers of the atmosphere for the data collected from the Indian MST Radar. People carry out their analysis assuming that the noise is Gaussian and in fact, in most of the scenarios, the noise is Gaussian. There is a much chance of getting inaccurate results if it is not. Gaussianity tests namely Autocorrelation (AC) and Power Spectral Density (PSD) tests are conducted to find whether the noise is Gaussian or not. In non-Gaussian cases, further analysis is carried out using Empirical Mode Decomposition (EMD). Once the exact type of noise contained in the data is known, specific denoising techniques can be applied so as to get better results. We develop the energy models of various noise distributions using EMD, test on random sequences, exponentials and derive the characteristics under various environments. Finally, the developed models are compared with the models obtained with the radar data and noise characterization is done.

Keywords: MST Radar, Noise Modelling, Wavelet Based Denoising, Principal Component Analysis, Gaussianity tests, Empirical Mode Decomposition, Intrinsic Mode Function

I. INTRODUCTION

Major advancements have been made in the radar probing of the atmosphere in early seventies through the pioneering work of Woodman and Guillen [1]. It led to explore the entire Mesosphere - Stratosphere - Troposphere (MST) region by means of high power VHF backscatter operating ideally around 50MHz. The concept of MST radar has been evolved from this idea and has been proved to be an excellent system in exploring the dynamics of middle and upper layers of atmosphere. The National MST Radar Facility (NMRF) has been established at Gadanki ($13.5^0\ N, 79.2^0\ E$) in India is used for the purpose of atmospheric probing in the MST regions. The Indian MST radar is highly sensitive, pulse-coded, coherent VHF phased array radar [2] [3] operating at 53MHz with a peak power-aperture product of $3X10^{10}\ Wm^2$. The echoes received from MST region represent atmospheric background information and is considered to be generated through a random process. The data are collected by the radar from multiple beam positions (East, West, North, South, Zenith-X and Zenith-Y). In the atmosphere, turbulence can be thought of as random motion of a fluid thus causing variations in the refractive index.

The main purpose of Indian MST radar is to study winds, waves, turbulence and estimate the wind parameters by using the echoes obtained over the height range of 1-100 km. In this paper, the data collected on June 9, 2006 over the range from 3.6 km to 25.6 km above the earth's surface with 150m resolution are taken. The echoes received from the heights below 50 km arise primarily due to neutral turbulence and above that height is due to irregularities in the electron density. In the height range of 30-60 km, atmosphere density as well as electron density are very low resulting in very weak echoes. The efficiency of the radar system depends on how best it can identify the echoes in the presence of noise and unwanted clutter. Spectral analysis techniques are applied to the data to estimate the Doppler spectrum in which some of the steps will be carried out in on-line and some in off-line. The data input to the processing system is in complex format obtained after decoding and coherent integrations. FFT is applied to the complex time-series data and power spectra is produced for each range bin in on-line processing while parameter extraction is done in off-line.

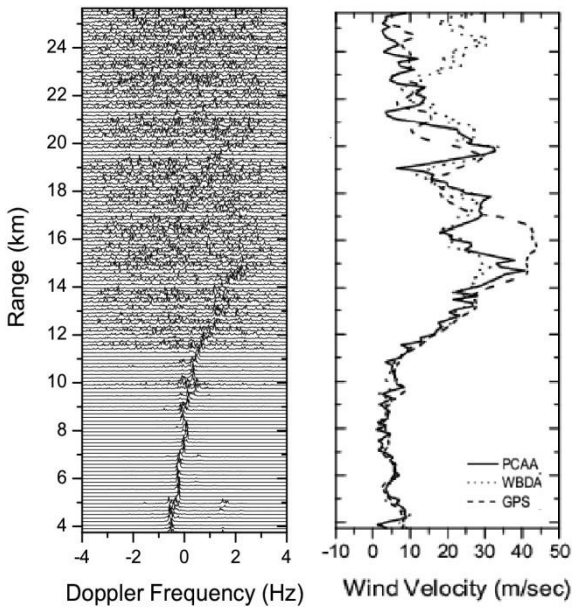

Fig. 1 (a) Typical Spectra of the East beam using PCA (b) Estimation of Wind velocity using WBD and PCA for radar data

Fig. 1a shows the spectrum of the East beam using Principal Component Analysis (PCA). The left side axis indicates the range (km) and is divided into 147 bins. For convenience, the total number of bins is characterized into three levels: lower bins numbered from 1 to 50, middle bins numbered from 51-100 and upper bins numbered from 101-147. It is observed that the lower bins of the atmosphere are noise-free and Doppler frequencies can be found easily. The spectrum in the middle and upper layers is dominated with noise. Several denoising techniques exist that can be applied in order to obtain a smooth

ISSN (Online) 2321 – 2004
ISSN (Print) 2321 – 5526

INTERNATIONAL JOURNAL OF INNOVATIVE RESEARCH IN ELECTRICAL, ELECTRONICS, INSTRUMENTATION AND CONTROL ENGINEERING
Vol. 2, Issue 4, April 2014

Doppler such that wind parameters can be estimated accurately if the noise added is Gaussian. Such denoising techniques are Wavelet Based Denoising (WBD) [4] and Principal Component Analysis (PCA). Fig. 1b shows wind velocity estimates using WBD and PCA and compared against the profile obtained using GPS sonde. There is a much variation in estimations at the middle layers as the applied WBD and PCA employ Gaussian based denoising techniques. Since the data has been probed through different layers of atmosphere, it cannot be made sure that the noise added to the echoes is Gaussian. It may be one or mixture of noise distributions that exist in nature. So, if the noise distribution is explored, better results can be obtained. By central limit theorem, the distribution is Gaussian in most of the cases and denoising techniques are applied accordingly.

In this paper, we first find whether the distribution is Gaussian or not using Gaussianity tests. The tests are described in Section II. If it is found to be non-Gaussian, we try to find the noise distribution using EMD which is described in Section III. For this purpose, energy models using EMD are developed for the simulated signals such as exponentials as well as random sequences and are compared with the models obtained with the radar data. Results are discussed in Section IV.

II. TESTS FOR GAUSSIANITY

The modelling of real-world signals is discussed in [5]. The objective of signal modelling is to consider some sample sequence of a signal, estimate the model parameters such that it has to satisfy prescribed criterion. In the first step, the model is to be fitted followed by the validation of the model so as to fit with the key features of data considered.

Autocorrelation test When the length of the data sequence N is large enough, the distribution of the estimated autocorrelation coefficients $\hat{p}(l) = \hat{r}(l)/r(0)$ is approximately Gaussian with zero mean and variance of $1/N$ [6]. The approximate 95 percent confidence limits are $\pm 1.96/\sqrt{N}$. Any estimated values of $\hat{p}(l)$ that fall outside these limits are significantly different from zero with 95 percent confidence. The values that cross confidence limits indicate nonwhiteness of the residual signal.

Power Spectral Density test The standardized cumulative Periodogram of a random sequence of length N is defined by

$$\tilde{I}(k) \triangleq \begin{cases} 0, & k < 1 \\ \dfrac{\sum_{i=1}^{k} \hat{R}(e^{j2\pi i/N})}{\sum_{i=1}^{K} \hat{R}(e^{j2\pi i/N})}, & 1 \le k \le K \\ 1, & k > K \end{cases}$$

where K is the integer part of $N/2$. If the process is White Gaussian, then the random variables $\tilde{I}(k)$, $k = 1,2, \ldots \ldots \ldots, K$ are independently and uniformly distributed in the interval (0, 1). The plot of $\tilde{I}(k)$ should be approximately linear with respect to k. The hypothesis is rejected at level 0.05 if $\tilde{I}(k)$ exits the boundaries specified by

$$\tilde{I}^{(b)}(k) = \frac{k-1}{K-1} \pm 1.36(K-1)^{-\frac{1}{2}} \quad 1 \le k \le K$$

The tests are performed on Gaussian noise and exponentials with SNRs of 10dB and -10dB. Results are shown in Fig. 2. The vertical solid lines of Fig. 2a indicate the amplitude levels of estimated autocorrelation coefficients $\hat{p}(l)$ plotted against *lag*, solid line of Fig. 2b indicates $\tilde{I}(k)$ plotted as the function of normalized frequency and the dashed lines in both indicate the confidence limits. The first coefficient at lag 0 will be unity in all the cases. If all the remaining solid lines fall within the limits, it indicates Gaussianity. The same applies to PSD test also. In the case of noise-only signal, all the solid lines in Fig. 2a and 2b fall within dashed lines as expected. If it is pure signal, those lines cross the dotted lines indicate the non-Gaussianity. In case of 10dB noisy signal where signal dominates noise, the tests still indicate nonwhiteness. But, for a -10dB noisy signal, the tests indicate the Gaussianity although the signal contains a frequency. From the analysis made, it can be concluded that the tests show the presence of Gaussianity if the signal has an SNR less than -10dB even though it contains a frequency.

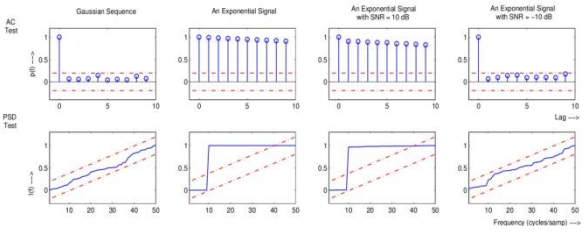

Fig. 2 Autocorrelation and PSD tests on deterministic signals

The tests are applied on radar data for all the beams at different levels: lower, middle and upper bins. The results are shown in Fig. 3 of one bin each at three levels for all the beams. It is inferred that at lower bins up to 50, there is no case of Gaussianity and at higher bins from bin numbered 116, Gaussianity begins in all the beams. In the upper middle bins, i.e. above 75th bin, Gaussianity begins in non-vertical beams and no Gaussianity in the vertical beams. But, from Fig. 4, some bins show non-Gaussianity in non-vertical beams as it is expected to be Gaussian, which are termed as *Ambiguity Bins*. It can't be concluded with these tests that whether Gaussianity exists or not as several algorithms fail at those bins and thus get inaccurate wind speeds. Special attention is to be paid to determine the noise distribution so as to get better results by applying appropriate denoising techniques. To this end, we go for a data analysis technique called Empirical Mode Decomposition and significant conclusions are drawn.

ISSN (Online) 2321 – 2004
ISSN (Print) 2321 – 5526

INTERNATIONAL JOURNAL OF INNOVATIVE RESEARCH IN ELECTRICAL, ELECTRONICS, INSTRUMENTATION AND CONTROL ENGINEERING
Vol. 2, Issue 4, April 2014

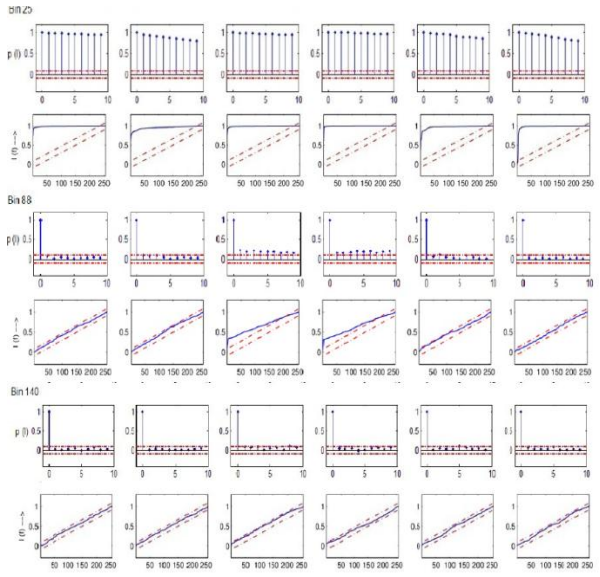

Fig. 3 Autocorrelation and PSD tests on radar data for bins 25, 80 and 140.

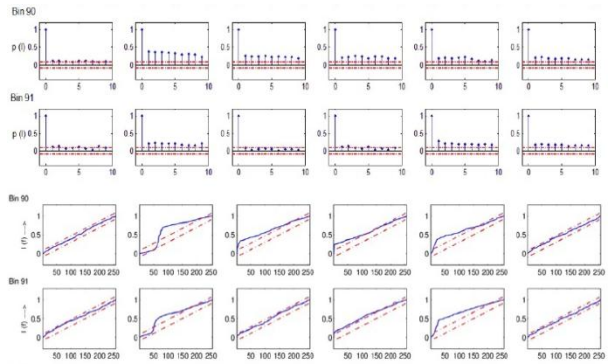

Fig. 4 Ambiguity cases on application of Autocorrelation and PSD tests on radar data for bins 90 and 91

III. EMPIRICAL MODE DECOMPOSITION

Traditional EMD: Since there exists an ambiguity in concluding that the noise in the upper middle bins is Gaussian, the noise distribution is analysed using EMD in this section. EMD localizes any event on both time as well as frequency scales. A signal is decomposed into a number of Intrinsic Mode Functions (IMFs) [7] based on energy extraction associated with various intrinsic time scales. From the Hilbert transform of these IMFs, instantaneous frequencies can be calculated. For an arbitrary time series $X(t)$, Hilbert transform $Y(t)$ is defined as

$$Y(t) = \frac{1}{\pi} P \int_{-\infty}^{\infty} \frac{X(t')}{t - t'} dt' \quad (1)$$

where P indicates the Cauchy principal value. With this definition, $X(t)$ and $Y(t)$ form the complex conjugate pair and we can have an analytic signal $Z(t)$ as

$$Z(t) = X(t) + iY(t) = a(t)e^{i\theta(t)} \quad (2)$$

where

$$a(t) = [X^2(t) + Y^2(t)]^{1/2} \text{ and } \theta(t) = \tan^{-1}\left(\frac{Y(t)}{X(t)}\right) \quad (3)$$

Equation (1) defines the Hilbert transform as the convolution of $X(t)$ with $1/t$ and the polar coordinate expression (2) represents the local nature of (1). With the Hilbert transform, the instantaneous frequency is defined as,

$$\omega = \frac{d\theta}{dt} \quad (4)$$

For defining the instantaneous frequency, the necessary condition is that the functions should be symmetric with respect to local zero mean and have the same number of zero crossings and extrema. Thus, the concept of IMF came into existence. The name is adopted so because it represents the oscillation mode embedded in the data. A function is said to be an IMF if it satisfies the following two conditions:

1. The number of extrema and the number of zero crossings must either equal or differ at most by one and

2. The mean value of the envelopes defined by the local maxima and the local minima is zero.

The description of the conditions is defined in [7]. But, most of the data are not IMFs. At any given time, the data may involve more than one oscillatory mode and that is why the simple Hilbert transform cannot provide the full description of the frequency content for the general data [8]. The EMD is based on the following assumptions:

1. The signal has at least two extrema: one maximum and one minimum

2. The characteristic time scale is defined by the time lapse between the extrema and

3. If the data were totally devoid of extrema but contained only inflection points, then it can be differentiated once or more times to reveal the extrema.

Let us consider EMD decomposition for the data $X(t)$. The decomposition method starts with defining the local maxima and local minima. All the local maxima and local minima are connected by two different envelopes such that entire data is covered in between them. Let m_1 be the mean of the two envelope and h_1 be the difference between the data $X(t)$ and mean m_1 which is expressed mathematically as,

$$X(t) - m_1 = h_1 \quad (5)$$

This is first sifting. h_1 is the first component decomposed from the signal which should be an IMF ideally. But, overshoots and undershoots occur which can generate the new extrema. So, sifting process is done again considering h_1 as data and is represented as,

$$h_1 - m_{11} = h_{11} \quad (6)$$

where m_{11} be the mean of the envelopes defined for h_1. Still h_{11} may not be an IMF. Sifting process is repeated k

ISSN (Online) 2321 – 2004
ISSN (Print) 2321 – 5526

INTERNATIONAL JOURNAL OF INNOVATIVE RESEARCH IN ELECTRICAL, ELECTRONICS, INSTRUMENTATION AND CONTROL ENGINEERING
Vol. 2, Issue 4, April 2014

times until h_{1k} is an IMF. The kth component is defined as,

$$h_{1(k-1)} - m_{1k} = h_{1k} \quad (7)$$

Thus, the first IMF component from the data is designated as,

$$c_1 = h_{1k} \quad (8)$$

Now, c_1 can be separated from the data by,

$$X(t) - c_1 = r_1 \quad (9)$$

where r_1 is the residue which still contains information of longer period components. Now, it is treated as the new data and is subjected to same sifting process (steps [5] to [8]). The process is repeated on all the subsequent $r_j s$ as,

$$r_1 - c_2 = r_2, r_2 - c_3 = r_3, \dots\dots, \ r_{n-1} - c_n = r_n \quad (10)$$

The sifting process is stopped when any of the following criteria occurs:

1. When either the component c_n or the residue r_n becomes less than the predetermined value or

2. When the residue r_n becomes a monotonic function from which no IMF can be extracted.

By the decomposed IMF components, data $X(t)$ can be expressed as the linear combination of n-empirical modes and a residue r_n as

$$X(t) = \sum_{i=1}^{n} c_i + r_n \quad (11)$$

All the steps involved in EMD decomposition are shown in Fig. 5.

Complex EMD (CEMD): The traditional EMD explained above is applicable only for real-valued data. There is need in developing EMD for complex time-series data because in practical areas like sonar radar, telecommunications etc., complex-valued data is used. A method for complex-data has been proposed [9]. The basic idea behind the development of CEMD is that: a) it behaves as a dyadic sub band decomposition structure [10] b) divide the complex signal into its positive and negative frequency parts and derive the relation between them. The CEMD for $x[n]$ can be expressed as,

$$x[n] = \sum_{i=-N_-, i\neq 0}^{N_+} y_i[n] + r[n] \quad (12)$$

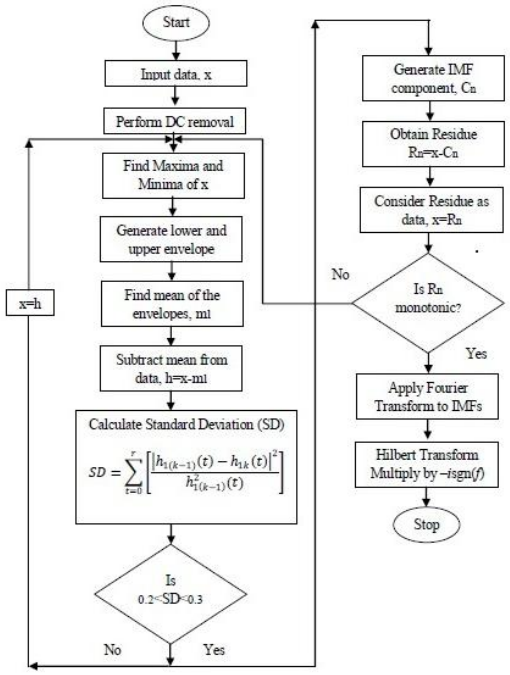

Fig. 5 Steps involved in classical EMD

where

$$y_i[n] = \begin{cases} \left(x_i[n] + j\mathcal{H}\left[x_i[n]\right]\right) & i = 1, \dots\dots, N_+ \\ \left(x_i[n] + j\mathcal{H}\left[x_i[n]\right]\right)^* & i = -N_-, \dots\dots, -1 \end{cases} \quad (13)$$

is the i^{th} complex IMF and $r[n]$ represents a trend within the data set. We apply CEMD to study the characteristics of Gaussian noise. For this, a set of 1000 independent Gaussian complex-valued time series of 512 samples is generated. The power spectra of IMFs generated from these complex-valued time series data are analyzed and the resulting spectra are averaged. Fig. [6] depicts the averaged spectra for the first seven IMFs in both the negative and positive frequency range. The idea behind this simulation is to understand that CEMD decomposes broadband noise.

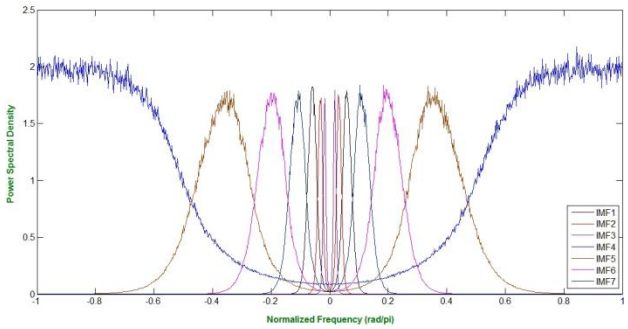

Fig. 6 Complex-valued EMD and the equivalent filters within a filter bank

Bivariate EMD (BEMD) Although CEMD decomposes noise well, treating the positive and negative frequency components as two separate independent signals results in loss of information in the signal as they are mutually dependent. Also, the division into positive and negative

ISSN (Online) 2321 – 2004
ISSN (Print) 2321 – 5526

INTERNATIONAL JOURNAL OF INNOVATIVE RESEARCH IN ELECTRICAL, ELECTRONICS, INSTRUMENTATION AND CONTROL ENGINEERING
Vol. 2, Issue 4, April 2014

frequency components creates an ambiguity at the zero frequency. It also cannot be extended to higher-dimensional cases. To overcome all the above, BEMD has been proposed [11] which decomposes a complex signal with traditional EMD by operating completely in C. The merits of BEMD over CEMD are that of no need of splitting the signal into two parts, can be extended to higher dimensional cases and no ambiguity case at zero frequency. Traditional EMD is based on the notion of *oscillation* where as BEMD is based on the notion of *rotation*. The basic idea behind the BEMD development is that *bivariate signal = fast rotations superimposed on slower rotations* [11]. The slowly rotating component is defined as the mean of envelope which is three-dimensional tube that encloses the signal. The slowly rotating portion of the signal at any point in time can be defined as the center of the enclosing tube. For defining the center, only a given number of points on the tube's periphery are considered, each one being associated with a specific direction. Any number of points is considered. For example, if four points are taken, they can be the extreme points in *top*, *bottom*, *left* and *right* directions. The point in each direction is defined in a unique way, for example, the top point is defined only when the signal reaches a local maximum in the vertical direction and is also tangent to the top of the tube. With this, the mean of the envelope is defined as the intersection of two straight lines, one being halfway between the two horizontal tangents and the other one being halfway between the two vertical tangents as shown in Fig. 7.

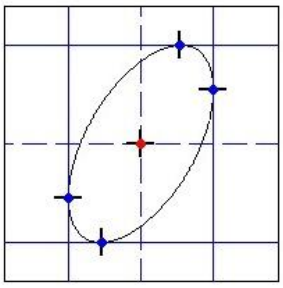

Fig. 7 Mean Definition of Envelope in BEMD

Let $\varphi_k = {2k\pi}/{N}, 1 \le k \le N$ be the set of directions with N being the number of directions. BEMD is in concept same as that of traditional EMD except that two new sifting elementary operators S^{B1} and S^{B2} are introduced [11] and the algorithmic steps given in [11] are presented below for completeness.

Algorithm 1

1. For each direction $k \in [1, N]$,

1.a. Project the complex-valued signal $x(t)$ on direction φ_k: $p_{\varphi_k}(t) = Re\,(e^{-i\varphi_k} x(t))$

1.b. Extract the locations t_i^k of the maxima of $p_{\varphi_k}(t)$

1.c. Interpolate the set $(t_i^k, x(t_i^k))$ to obtain the envelope curve in direction φ_k: $e_{\varphi_k}(t)$.

2. Compute the mean of all the envelope curves: $m(t) = \frac{1}{N}\sum_k e_{\varphi_k}(t)$.

3. Subtract the mean to obtain $S^{B1}[x](t) = x(t) - m(t)$.

Algorithm 2

1. For each direction $k \in [1, N]$,

1.a. Project the complex-valued signal $x(t)$ on direction φ_k: $p_{\varphi_k}(t) = Re\,(e^{-i\varphi_k} x(t))$.

1.b. Extract the maxima of $p_{\varphi_k}(t)$: t_i^k, p_i^k.

1.c. Interpolate the set $(t_i^k, e^{i\varphi_k} p_i^k)$ to obtain the partial envelope curve in direction φ_k: $e_{\varphi_k}^1(t)$.

2. Compute the mean of all tangents: $m(t) = \frac{2}{N}\sum_k e_{\varphi_k}^1(t)$.

3. Subtract the mean to obtain $S^{B2}[x](t) = x(t) - m(t)$.

Algorithm 2 is further simplified to *Algorithm 3* as below:

Algorithm 3

1. For each direction $k \in [1, N/2]$,

1.a. Project the complex-valued signal $x(t)$ on direction φ_k: $p_{\varphi_k}(t) = Re\,(e^{-i\varphi_k} x(t))$.

1.b. Compute the partial estimate in direction φ_k: $s_{\varphi_k}(t) = e^{i\varphi_k} S[p_{\varphi_k}](t)$.

2. Compute the final estimate: $S^{B2}[x](t) = \frac{2}{N}\sum_k s_{\varphi_k}(t)$.

IV. NOISE MODELLING

Theoretical models

The driving idea of the present paper is that if the energies of the IMFs resulting from the decomposition of a noise-only signal are known, then in actual cases of radar signals comprising of both information and noise, noise can be characterized and separated such that further analysis is carried out on the resulting denoised signal. In the present context, we restrict to noise characterization only. The power spectra of noisy IMFs exhibit the same characteristics as those obtained with any dyadic filter structure. Thus, the IMF energies should linearly decrease with respect to the IMF number [12]. In this paper, we consider the following distributions: *Gaussian, Rayleigh, Cauchy, Laplace* and *Weibull* for modelling the noise in the radar data. Since the length of complex time series of each bin of the raw data is 512, we take the same number of Uniform random variables distributed in the interval (0,1) and generate the above mentioned distributions using standard transformations. BEMD is applied for the distributions, IMFs are generated and energies are calculated. As the IMFs are complex-valued, energy models are developed for three different cases: directly obtained complex IMFs, real part of complex IMFs and imaginary part of complex IMFs. Thus, 1000 Monte Carlo simulations are run, find the average energies and the same are plotted as shown in Fig. 8.

ISSN (Online) 2321 – 2004
ISSN (Print) 2321 – 5526

INTERNATIONAL JOURNAL OF INNOVATIVE RESEARCH IN ELECTRICAL, ELECTRONICS, INSTRUMENTATION AND CONTROL ENGINEERING
Vol. 2, Issue 4, April 2014

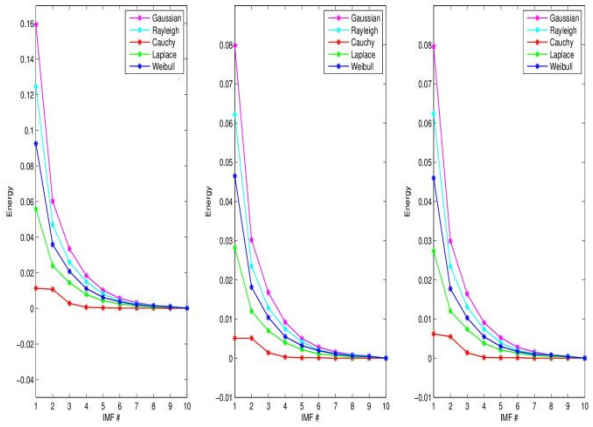

Fig. 8 Energy Models of Various Distrıcutions (a) Complex IMF Energy Model (b) Real Part Energy Model and (c) Imaginary Part Energy Model

Testing the models on exponentials

Before applying to the radar data, the developed energy models are tested on the same test signals taken in section II. The results are as shown in Fig. 9. When BEMD is applied to a pure exponential, it results in a single IMF as all the oscillations are constrained in the first IMF itself. The energy of IMF is far greater than that of energy of first IMF of the developed energy models. This type of plot tells us that signal is pure and consists of a single frequency. When BEMD results in more than one IMF, the signal may be noisy signal or consists of more than one frequency. For a signal with 10dB SNR, BEMD results in a few IMFs. From the energy model, it is seen that signal is in second IMF as its energy point deviates from the regular noise model developed. The energies of remaining IMFs are in concurrence with the developed model indicating that the noise containing in those IMFs is Gaussian. At this point, we stand at two different conclusions: signal is present in only second IMF and is taken as denoised signal or the noise in the signal is characterized as Gaussian. The same occurs with 0dB SNR signal also. But, signal is in third IMF now and also more number of IMFs results as compared to second case because oscillations will be present more when noise increases. For a -10dB test signal, the obtained energy model follows the same trend as that of developed noise model of Gaussian since noise dominates the signal. Signal of very low strength is found in third IMF. From the plots, it is clearly seen that if BEMD is applied on a signal consisting of Gaussian noise, the resulting Energy-IMF# model conveys that noise present is Gaussain and also tells us which IMFs consist of Gaussian noise. The same is applicable to all other distributions.

Testing the models on radar signals

In the similar manner, we apply BEMD to the radar dara for ambiguity bins. The results are shown in Fig. 10 using complex IMF energy model for bin numbered 90. Although, results for only one bin are shown, the same trends are obtained almost in every ambiguity bin for all hree developed models: complex, real and imaginary Energy-IMF# models. So, only complex energy model is shown. In very few cases, results obtained are a bit different. Consider the north beam of bin numbered 91 for which results are shown in Fig. 11. The overall complex

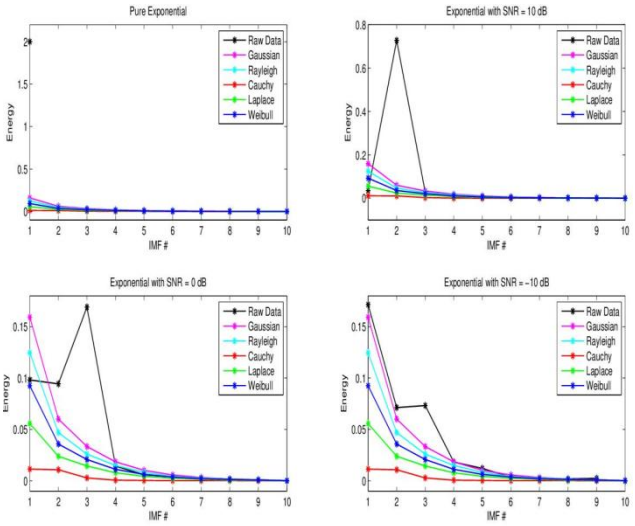

Fig. 9 Testing of Energy Models on Simulated signals with complex IMF Energy Model

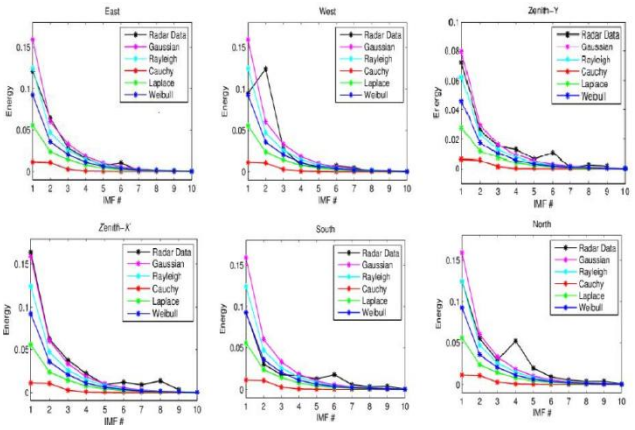

Fig. 10 Testing of Energy Models on Radar data with complex IMF Energy Model for bin 90

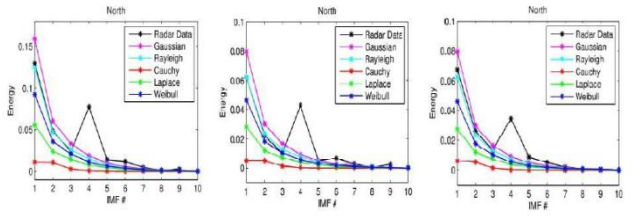

Fig. 11 Testing of Energy Models on Radar data with complex, real and imaginary IMF Energy Models for bin 91

energy model shows Rayleigh distribution whereas the real and imaginary energy models show Weibull and Rayleigh distributions respectively. It may be viewed that imaginary part is more contributing than the real part of the complex radar data in these particular cases. But, on the whole, we have to concentrate on the complex energy model. Only first few IMFs are to be considered more to find whether the noise in radar data being under test is

ISSN (Online) 2321 – 2004
ISSN (Print) 2321 – 5526

INTERNATIONAL JOURNAL OF INNOVATIVE RESEARCH IN ELECTRICAL, ELECTRONICS, INSTRUMENTATION AND CONTROL ENGINEERING
Vol. 2, Issue 4, April 2014

following any trend with the developed models. The reason is that noise is contained in the first few IMFs and signal is present in the remaining IMFs, if any, as seen in case of simulated signals. From the overall analysis carried out on ambiguity bins for data on different dates and scans, it is seen that non-vertical beams East and North follow Rayleigh distribution, West and South beams follow Weibull distribution, vertical beams Zenith-X and Zenith-Y follow Gaussian distribution. Thus, noise characterization in ambiguity bins where the noise is expected to be other than Gaussian is realized in this paper.

V. CONCLUSION

We characterize the noise present in the radar data and significant conclusions are drawn. With the derived noise characterization, certain techniques can be applied to the noisy radar signal to reconstruct the signal in order to estimate the wind parameters more accurately. The analysis is carried out for data collected on different days of all beams and scans. The work can be extended by automating the characterization as well as reconstruction of the signal.

ACKNOWLEDGMENT

We would like to thank Department of Science and Technology (DST) for providing financial assistance and also National Atmospheric Research Laboratory (NARL), Gadanki for providing radar data and technical assistance.

REFERENCES

[1] Ronald F. Woodman and Alberto Guillen, "Radar Observations of Winds and Turbulence in the Stratosphere and Mesosphere", J.Atmos.Sci., vol. 31, pp. 493-505, Mar. 1974.
[2] P. B. Rao, A. R. Jain, P. Kishore, P. Balamuralidhar, S. H. Damle and G. Viswanathan, "Indian MST radar-1. System description and simple vector wind measurements in ST", Radio Sci., vol. 30, no. 4, pp. 1125-1138, Jul-Aug. 1995.
[3] A. R. Jain, Y. Jaya Rao, P. B. Rao, V. K. Anandan, S. H. Damle, P. Balamuralidhar, Anil Kulakarni and G. Viswanathan, "Indian MST radar 2. First scientific results in ST mode", Radio Sci., vol. 30, no. 4, pp. 1139-1158, Jul-Aug. 1995.
[4] Sreenivasulu Reddy Thatiparthi, Ramachandra Reddy Gudheti and Varadarajan Sourirajan, "MST Radar Signal Processing Using Wavelet-Based Denoising", IEEE Geoscience and Remote Sensing Letters, vol. 6, no. 4, pp. 752-756, Oct. 2009.
[5] Dimitris G. Monolakis, Vinay K. Ingle and Stephen M. Kogon, Statistical and adaptive signal processing, Artech House, 2005.
[6] Kendall M.G. and A. Stuart, Advanced Theory of Statistics, Macmillan Publishing Company, 1983.
[7] Norden E. Haung, Zheng Shen, Steven R. Long, Manli C. Wu, Hsing H. Shih, Quanan Zheng, Nai-Chyuan Yen, Chi Chao Tung and Henry H.Liu, The empirical mode decomposition and the Hilbert spectrum for nonlinear and non-stationary time series analysis, Proc. R. Soc. Lond., pp. 903-995, 1998.
[8] Long S.R., Huang N.E., Tung C.C., Wu M.L., Lin R.Q., Mollo-Christensen E. and Yuan Y., The Hilbert Techniques: An Alternate Approach for Non-Steady Time Series Analysis, IEEE Geoscience Remote Sensing Soc. Lett., vol. 3, pp. 6-11, 1995.
[9] Toshihisa Tanaka and Danilo P. Mandic, Complex Empirical Mode Decomposition, IEEE Signal Process. Lett., vol. 14, no. 2, pp. 101-104, Feb. 2007.
[10] Patrick Flandrin, Gabriel Rilling and Paulo Goncalves, Empirical Mode Decomposition as a Filter Bank, IEEE Signal Process. Lett., vol. 11, no. 2, pp. 112-114, Feb. 2004.
[11] Gabriel Rilling, Patrick Flandrin, Paulo Goncalves abd Jonathan M. Lilly, Bivariate Empirical Mode Decomposition, IEEE Signal Process. Lett., vol. 14, no. 12, pp. 936-939, Dec. 2007.
[12] Yannis Kopsinis and Stephen McLaughlin, Development of EMD-Based Denoising methods Inspired by Wavelet Thresholding, IEEE Trans. Signal Process., vol. 57, no. 4, pp. 1351-1362, Apr. 2009.

BIOGRAPHY

Uma Maheswara Rao Damarapati received his B.Tech. degree in ECE from SIETK in 2010 and M.Tech. degree in Communication Engineering from VIT University in 2012. He secured University 3rd rank in B.Tech. over all affiliated colleges of JNTU and received gold medal from VIT University in M.Tech. He also got first prize twice for the two papers presented by in First and Second International Science, Engineering and Technology (SET) conferences held by VIT University biannually. He got two times merit scholarship and endowment award from chancellor of VIT University. He worked as Junior Research Fellow from June, 2011 to May, 2012 and is working as Project Engineer in Wipro Limited till date.

T. Sreenivasulu Reddy received the B.Tech. degree in ECE from Sri Venkateswara University, Tirupati, India, in 1990, the M.Eng. degree in digital electronics from Karnatak University, Dharwad, India, in 1996 and Ph.D. degree in Radar Signal Processing from Sri Venkateswara University, Tirupati. He is currently an Associate Professor with the Department of Electronics and Communication Engineering, College of Engineering, Sri Venkateswara University. His research interests include radar and image signal processing. Mr. Reddy is a Fellow of the Institution of Electronics and Telecommunication Engineers and a member of the Indian Society for Technical Education.

G. Ramachandra Reddy received the M.Sc. and M.Sc.(Tech.) degrees from the Birla Institute of Technology and Science, Pilani, India, in 1973 and 1975, respectively, and the Ph.D. degree from the Indian Institute of Technology, Madras, India, in 1987. In 1976, he joined the Department of Electrical and Electronics Engineering, College of Engineering, Sri Venkateswara University, Tirupati, India, and worked till 2010. He is currently Senior Professor in VIT University, Vellore. Also, he is holding the position of dean for the School of Electronics Engineering and Accreditation and Academic Committee. From February 1989 to May 1991, he was with the Department of Electrical and Computer Engineering, Concordia University, Montreal, QC, Canada, as a Visiting Scientist. Dr. Ramachandra Reddy is a Fellow of the Institution of Electronics and Telecommunication Engineers and a member of the Indian Society for Technical Education.